Entrainment in the Crown Region of Forced Turbulent Fountains

L. A. Awin[1], S. W. Armfield[1], M. P. Kirkpatrick[1], N. Williamson[1] and W. Lin[2]

[1]School of Aerospace, Mechanical and Mechatronic Engineering
The University of Sydney, New South Wales 2006, Australia

[2]College of Science and Engineering
James Cook University, Townsville, Queensland 4811, Australia

Abstract

Entrainment from the ambient into the crown region of forced turbulent fountains is examined using numerical simulation for Reynolds numbers $2000 \leq Re \leq 3500$ and Froude numbers $5 \leq Fr \leq 24$, where Re and Fr are based on the fountain source properties. The fountain flow consists of three regions, the inner upflow, outer downflow, and the crown where the inner upflow transitions to the outer downflow. The results indicate that the crown region entrainment volume flux is relatively insensitive to the Reynolds number in the fully turbulent fountain regime ($Re \geq 2000$), while it has a linear relation with the Froude number for the cases considered, similar to that of the mean penetration height for forced fountains ($Fr \geq 3$). Linear regression of the results for the crown entrainment give the relation as $Q_E/Q_o =$ 0.1721 Fr + 0.705, where Q_E is the entrainment and Q_o is the fountain source volume flux.

Introduction

A fountain occurs when a dense fluid is projected upward into a less dense ambient. The rise of the dense jet fluid is opposed by buoyancy, and further limited by the entrainment of fluid from the ambient. The fountain structure consists of a core of rising fluid and a surrounding falling annular plume, with a crown region at the top where the rising fluid transitions to the descending annular plume. In the crown region, the inner upflow fluid which rises from the source, becomes stagnant at the maximum height, entrains surrounding ambient fluid and leaves the crown region to descend back to the source level as an outer downflow, as illustrated by the schematic in figure 1. Fountains occur widely in environmental and industrial settings. Volcanic eruptions, atmospheric convection, building ventilation and re-fueling fuel tanks are all examples where turbulent fountains occur and strongly influence the overall behaviour [2, 11, 3, 8].

Fountains may be classified by two non-dimensional numbers, the Reynolds number (Re) and the Froude number (Fr), defined below. For Reynolds numbers greater than 2000, the fountain is fully turbulent [17] and for Froude numbers greater than 3, the fountain is classified as forced [9]. Several studies have identified scaling relations for the mean fountain penetration height over a range of Froude numbers [2, 15, 9, 12, 7, 18, 4, 17]. For the forced fountain regime, the flow has a linear scaling $Z_m/R_o = CFr$, where C is a constant, Z_m is the mean fountain penetration height and R_o is the source radius. This linear scaling has been validated by several laboratory experiments and shown to be valid for $3 \leq Fr \leq 300$, although the constant C has been observed to vary between 2.1 and 3.06 [2, 15, 12, 7, 17].

Theoretical models for the fountain rise height have been developed by extending plume and jet models with the assumption that the lateral entrainment, that is the entrainment from the ambient into the outer downflow, and from the outer downflow into the inner upflow, will obey standard jet/plume like entrainment relations. These models were first applied to negatively buoy-
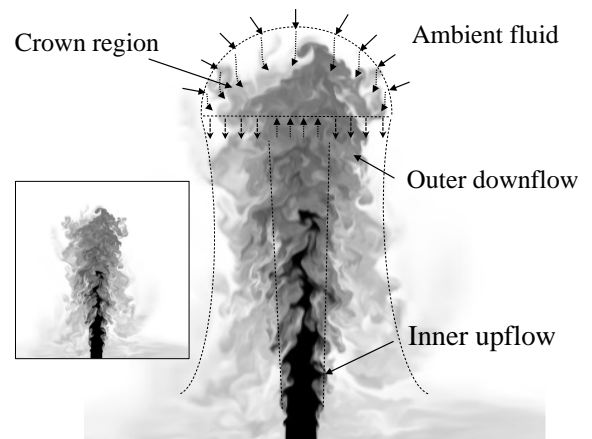
Figure 1: Schematic of a forced turbulent fountain.

ant starting jets, predicting a linear Froude number relation for the initial rise height [1, 13, 9]. This approach was later extended to predict the rise height of fully developed fountains by including the effect of the outer downflow, with similar entrainment assumptions [4], with the results validated against the experimental data of [12]. Detailed numerical results for the lateral entrainment were obtained by [16], showing that similarity based entrainment relations did not accurately predict the behaviour, and suggesting that the self-similarity assumptions embedded in the theoretical models were open to question.

Experimental measurements of total entrainment into turbulent forced fountains, that is the lateral entrainment plus the crown entrainment, found that the total entrainment $Q_E/Q_o =$ 0.71Fr [6], with Q_o the fountain source volume flux. Although no previous investigations have been carried out for the entrainment into the crown region only, an investigation of the similar flow of a negatively buoyant jet penetrating a density interface found the total entrainment for the high Froude number case to be $Q_E/Q_o =$ 0.42Fr, with approximately 20 % of the total entrainment occurring in the crown region [14].

The fountain rise height and overall behaviour is strongly dependent on the entrainment of the ambient fluid into the fountain, and the entrainment and mixing of the outer and inner flows. All the theoretical models include an estimate of the entrainment, typically based on jet and plume type entrainment laws. Despite this, there has been relatively little direct measurement of the entrainment, either experimentally or via direct numerical simulation, with no direct measurement or calculation of entrainment for the crown region. In this study we will conduct a numerical investigation of forced fountain flow, quantifying the entrainment into the crown region and establishing a Froude number based scaling relation.

Numerical Method

Results are obtained by solving the Navier-Stockes equations for incompressible flow, with the Oberbeck-Boussinesq approximation for buoyancy. The dimensionless continuity, momentum, and scalar transport equations are:

$$\frac{\partial u_i}{\partial x_i} = 0, \tag{1}$$

$$\frac{\partial u_i}{\partial t} + \frac{\partial (u_i u_j)}{\partial x_j} = -\frac{\partial p}{\partial x_i} + \frac{1}{Re}\frac{\partial^2 u_i}{\partial x_j \partial x_j} - \frac{\phi}{Fr^2}, \tag{2}$$

$$\frac{\partial \phi}{\partial t} + \frac{\partial (u_j \phi)}{\partial x_j} = \frac{1}{RePr}\frac{\partial^2 \phi}{\partial x_j \partial x_j}, \tag{3}$$

where $Re = V_o R_o/\nu$ is the Reynolds number, $Pr = \nu/\alpha$ is the Prandtl number, and $Fr = V_o/(g_o R_0)^{0.5}$ is the Froude number, all based on the source properties; velocity V_o, temperature θ_o, radius R_o, kinematic viscosity ν, thermal diffusivity α and reduced gravity $g_o = g(\rho_o - \rho_\infty)/\rho_\infty$, with ρ the density. The $._o$ and $._\infty$ subscripts indicate properties at the fountain source and in the ambient fluid, respectively. The dimensional velocity (U_i), temperature (θ), pressure (P), time (T) and length (X_i) are normalised as $u_i = U_i/V_o$, $\phi = (\theta - \theta_\infty)/(\theta_o - \theta_\infty)$, $p = P/(\rho V_o^2)$, $t = T/(R_o V_o)$ and $x_i = X_i/R_o$. The $._i$ subscript for u_i represents the three components of velocity $u_1 = u$, $u_2 = v$, $u_3 = w$ and for x_i represents the three dimensions in space $x_1 = x$, $x_2 = y$, $x_3 = z$.

The finite-volume method, implemented on a non-staggered Cartesian grid, is used to discretise the governing equations, with the ULTRA-QUICK limited scheme [5], used for the advection terms and all other spatial derivatives second-order. The transport equations are integrated in time using the Adams-Bashforth scheme for the advection terms and the Crank-Nicolson scheme for the diffusion terms. A fractional step method is used to obtain pressure and enforce continuity. A preconditioned Jacobi solver is used to invert the transport equations, and a preconditioned GMRES method to invert the pressure correction equation.

As shown in figure 2, the computational domain is a rectangular box where the top and side boundaries are open with zero normal-gradient boundary conditions on the velocity and scalar fields. The bottom boundary is a wall with no-slip and adiabatic conditions, except for the circular fountain source of radius $r = 1$, which is located in the centre, where the normal velocity and temperature have uniform profiles $v = 1$ and $\phi = -1$.

Results have been obtained for forced turbulent fountain flows with a range of Froude numbers $5 \leq Fr \leq 24$ and Reynolds numbers $2000 \leq Re \leq 3500$. The details of each of the simulation parameters are given in table 1. The grid size in the central region of the domain Δx, Δz, Δy is as given in table 1, where all x and z parameters are equal. Outside the central region, the grid is stretched towards the boundaries. The time step used for all simulations was set to ensure the Courant number lay between 0.25 and 0.35.

Results

Data sets for fully developed fountains with the properties in table 1 were generated. Figure 2 contains an instantaneous plot of a constant temperature surface for a typical fully developed fountain showing the complex and highly unsteady nature of the flow. Time averages of the fully developed flow were generated, with the time averaging interval located after start-up effects had died out, and with a large enough time averaging period to

$$\frac{\partial u}{\partial y} = \frac{\partial v}{\partial y} = \frac{\partial w}{\partial y} = 0,$$

Open boundary

$$\frac{\partial u}{\partial z} = \frac{\partial v}{\partial z} = \frac{\partial w}{\partial z} = 0,$$
Open boundary

$$\frac{\partial u}{\partial x} = \frac{\partial v}{\partial x} = \frac{\partial w}{\partial x} = 0,$$
Open boundary

Wall boundary

Source inlet boundary

$$u = v = w = 0, \frac{\partial \phi}{\partial y} = 0 \qquad u = w = 0, v = 1, \phi = -1$$
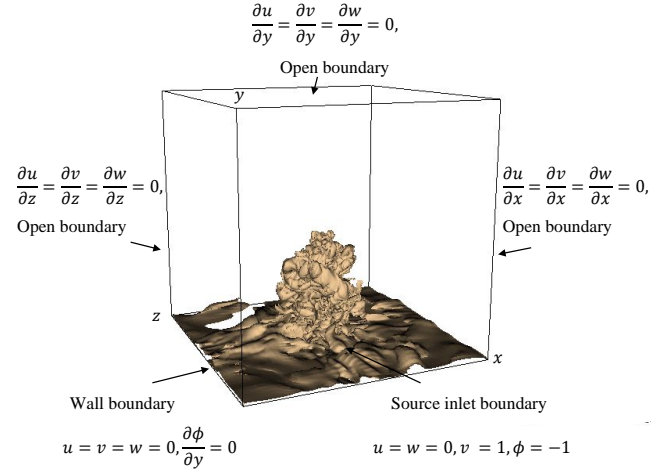
Figure 2: Domain and boundary conditions together with a constant temperature surface for a typical forced turbulent fountain.

Fr	Re	Pr	$\Delta x(\Delta z), \Delta y$	$L_x(L_z), L_y$	$N_x(N_z), N_y$
5	2500	1	0.04, 0.08	30,30	236, 265
5	3000	1	0.04, 0.08	30,30	236, 265
8	2500	1	0.04, 0.08	30,40	266, 350
8	3000	1	0.04, 0.08	30,40	266, 350
10	3500	1	0.04, 0.08	50,50	300, 400
12	2000	1	0.04, 0.08	50,60	330, 503
12	2750	1	0.04, 0.08	50,60	330, 503
12	3500	1	0.04, 0.08	50,60	330, 503
14	3000	1	0.04, 0.08	60,80	364, 550
16	3500	1	0.04, 0.08	60,80	394, 675
20	3000	1	0.04, 0.08	60,110	436, 800
24	3000	1	0.04, 0.08	80,120	486, 975

Table 1: $\Delta x, \Delta z, \Delta y$ are the finest grid size in the central region of the domain and $L_x, L_z, L_y, N_x, N_z, N_y$ are the domain size and number of nodes respectively.

ensure no windowing bias. The time average results are then used to obtain the entrainment volume flux of ambient fluid into the crown region.

Figure 3 contains zero contours of the time-averaged vertical velocity field. The time-averaged field is axisymmetric and the contours are plotted against r, the radius. Inside the contour the flow is rising, and outside it is falling. The rising flow initially expands with height reaching a maximum width marked by the arrows on figure 3 for each Fr and Re. The y-location of the maximum width is defined to be the location of the bottom boundary of the approximately hemispherical crown region. For $Fr = 5, 8, 14, 20$ at $Re = 3000$, the maximum widths are $r \approx 1.73, 2.32, 3.71, 4.99$ at heights $y \approx 6.5, 12.7, 23.2, 33.9$ respectively. For $Re = 2000, 2750, 3500$ at $Fr = 12$, the maximum width is $r \approx 3.16$ and the height is $y \approx 19.7$ for all. The overall structure is seen to vary with Fr, increasing in height and width, while having little dependence on Re, showing that at these fully turbulent Re values the flow is largely Re independent.

The zero velocity contour and the $\phi = -0.025$ temperature contour are plotted in figure 4 for the $Fr = 12$ and $Re = 2750$ case. As before the zero vertical velocity contour is the boundary between the inner upflow and the outer downflow. The $\phi = -0.025$ temperature contour is defined to be the boundary between the outer downflow and the ambient fluid. The inner
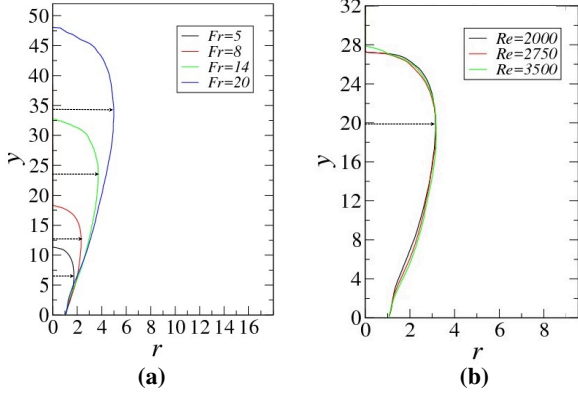
Figure 3: Zero contours of time-averaged vertical velocity for; (a) $Fr = 5, 8, 14, 20$ all at $Re = 3000$. (b) $Re = 2000, 2750, 3500$ all at $Fr = 12$.
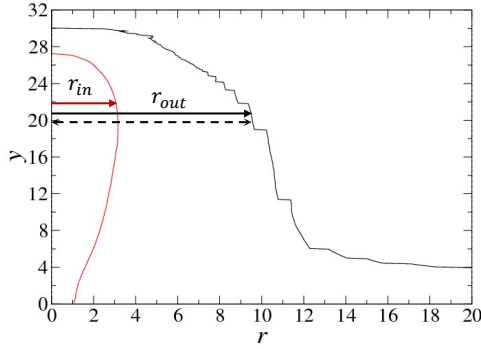
Figure 4: Zero velocity contours and $\phi = -0.025$ temperature contours for for $Fr = 12$ and $Re = 2750$. The red line is the boundary between the rising flow and falling flow and the black line is the boundary for the falling flow with the ambient fluid flow.

radius r_{in} is the radius of the rising fluid, and the outer radius, r_{out}, is the total radius of the fountain. The total crown region is then the region above the maximum r_{in} location, and inside the The $\phi = -0.025$ temperature contour.

The volume flux for the entrainment from the ambient into the crown region is then the difference between the volume flux of outer flow fluid exiting the crown region through the bottom, circular, surface of the region, and the volume flux of inner fluid entering the crown region through the bottom surface. That is the flux of Va_{out} minus the flux of Va_{in} as shown in figure 5. This is obtained by integrating the negative of the time average vertical velocity V_a over the bottom surface of the crown region:

$$Q_E = -2\pi \int_0^{r_{out}} V_a r dr \qquad (4)$$

Q_E, obtained as above for each case, is plotted against Fr in figure 6, with Q_E normalised by the source fountain flux Q_o. Also plotted on figure 6 is the best fit line obtained by linear regression,

$$\frac{Q_E}{Q_o} = 0.1721 Fr + 0.705 \qquad (5)$$
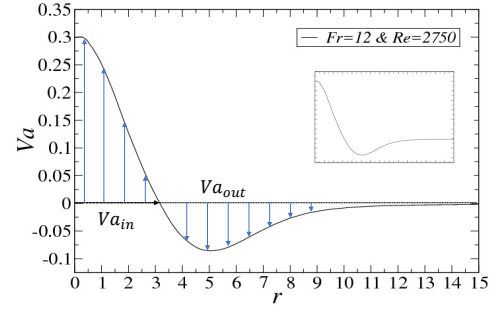
Figure 5: Vertical velocity profile at the radial location of the bottom boundary of the crown region. Va_{in} is the velocity profile rising flow and Va_{out} is the velocity profile of the falling flow.

with a fitting coefficient of $R^2 = 0.9686$. Overall the crown region entrainment rate is well approximated by this linear relation for the Fr range considered. Q_E has relatively little dependence on Reynolds number for the Re range considered. It is also apparent that the linear relation cannot be extended to zero Froude number, as that would imply a non-zero entrainment at $Fr = 0$.
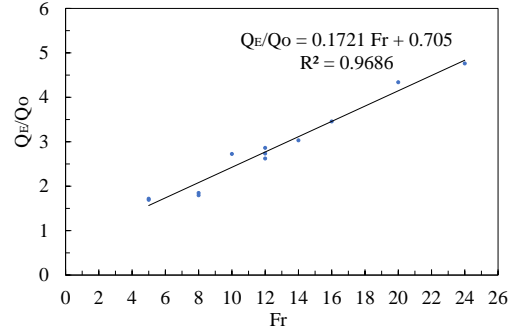
Figure 6: Linear scaling of the entrainment volume flux at the crown region of forced turbulent fountain. The sets of data of crown region volume flux compared with the Froude number.

Conclusions

Numerical simulations have been obtained for forced turbulent fountains over a range of Froude and Reynolds numbers. The fountains are characterised as having an inner upflow, an outer downflow, and a crown region in which the inner upflow transitions to the outer downflow. The boundary between the inner and outer flows was determined to be the zero contour of the time-average vertical velocity, with the bottom of the crown region being the height at which the radius of the zero contour, r_{in}, was maximum. The total fountain width was determined by the $\phi = -0.025$ temperature contour, and the crown region is that component of the domain lying above the bottom surface of the crown, and inside the $\phi = -0.025$ temperature contour. The entrainment volume flux was then obtained as the negative of the integral of the time-average vertical velocity over the bottom surface of the crown region.

The crown region entrainment volume flux was shown to be well approximated by a linear Froude number relation, obtained by linear regression. It is noted the scaling for the total entrain-

ment flux into the fountain, that is the sum of the crown and lateral fluxes, obtained by [6], was $Q_E/Q_o = 0.71Fr$, while in an investigation of the similar case of a negative buoyant jet penetrating a density interface, it was found that approximately 20% of the total entrainment was associated with the crown region [14]. 20% of 0.71 is 0.14, close to the crown entrainment scaling constant of 0.17 obtained in this investigation.

The linear relation included a constant of 0.705 implying a non-zero entrainment at Fr = 0, which is not physically possible. Fountains with Fr < 3 are classified as weak or very weak and have been shown to have different, non-linear, Froude number scalings for fountain height [9, 10]. It is expected that the crown region entrainment will also have different scalings for weak and very weak fountains and the scaling obtained here cannot be extended to Fr = 0.

Acknowledgements

References

[1] Abraham, G., Jets with negative buoyancy in homogeneous fluid, *J. Hydraul. Res.*, **5**, 1967, 235–248.

[2] Baines, W., Turner, J. and Campbell, I., Turbulent fountains in an open chamber. *J. Fluid Mech.*, **212**, 1990, 557–592.

[3] Branney, M.J. and Kokelaar, P., A reappraisal of ignimbrite emplacement: progressive aggradation and changes from particulate to non-particulate flow during emplacement of high-grade ignimbrite, *Bull. Volcanol.*, 1992, **54**, 504–520.

[4] Bloomfield, L. J. and Kerr, R. C., A theoretical model of a turbulent fountain, *J. Fluid Mech.*, **424**, 2000, 197–216.

[5] Bloomfield, L. J. and Kerr, R. C., Beyond first-order upwinding: the ULTRA-SHARP alternative for non-oscillatory steady state simulation of convection, *Int. J. Numer. Meth. Eng.*, **30**, 1990, 729–766.

[6] Burridge, H., and, Hunt, G., Entrainment by turbulent fountains, *J. Fluid Mech.*, **790**, 2016, 407–418.

[7] Campbell, I. H. and Turner, J. S., Fountains in magma chambers, *J. Petrol.*, **30**, 1989, 885–923.

[8] Friedman, P.D., Vadakoot, V.D., Meyer, W.J. and Carey, S., Instability threshold of a negatively buoyant fountain, *Exp. Fluids*, **42**, 2007, 751–759

[9] Kaye, N., and Hunt, G., Weak fountains, *J. Fluid Mech.*, **558**, 2006, 319–328.

[10] Lin, W., and Armfield, S. W., Very weak fountains in a homogeneous fluid, *Numer Heat Tr A Appl.*, **38**, 2000, 377-396.

[11] McDougall, T. J., Negatively buoyant vertical jets, *Tellus*, **33**, 1981, 313-320.

[12] Mizushina, T., Ogino, F., Takeuchi, H. and Ikawa, H., An experimental study of vertical turbulent jet with negative buoyancy, *Warme-und Stoffubertragung*, **16**, 1982, 15–21.

[13] Morton, B., Forced plumes, *J. Fluid Mech.*, **5**, 1959, 151–163.

[14] Shrinivas, A., and, G., Unconfined turbulent entrainment across density interfaces, *J. Fluid Mech.*, **757**, 2014, 573–598.

[15] Turner, J., Jets and plumes with negative or reversing buoyancy, *J. Fluid Mech.*, **26**, 1966, 779–792

[16] Williamson, N., Armfield, S. W., and Lin, W., Forced turbulent fountain flow behaviour, *J. Fluid Mech.*, **671**, 2011, 535–558.

[17] Williamson, N., Srinarayana, N., Armfield, S. W., Mcbain, G., and Lin, W., Low-Reynolds-number fountain behaviour, *J. Fluid Mech.*, **608**, 2008, 297–317.

[18] Zhang, H., and Baddour, R. E., Maximum penetration of vertical round dense jets at small and large Froude numbers, *J. Hydraul. Eng.*, **124**, 1998, 550–553.